AD_____

Award Number: DAMD17-99-1-9330

TITLE: Radiologist Evaluation of DEI Breast Specimen Imaging

PRINCIPAL INVESTIGATOR: Etta Pisano, M.D.

CONTRACTING ORGANIZATION: University of North Carolina
Chapel Hill, North Carolina 27599-7510

REPORT DATE: July 2000

TYPE OF REPORT: Annual

PREPARED FOR: U.S. Army Medical Research and Materiel Command
Fort Detrick, Maryland 21702-5012

DISTRIBUTION STATEMENT: Approved for Public Release;
Distribution Unlimited

The views, opinions and/or findings contained in this report are those of the author(s) and should not be construed as an official Department of the Army position, policy or decision unless so designated by other documentation.

REPORT DOCUMENTATION PAGE

Form Approved
OMB No. 074-0188

1. AGENCY USE ONLY (Leave blank)	2. REPORT DATE	3. REPORT TYPE AND DATES COVERED
	July 2000	Annual (1 Jul 99 - 30 Jun 00)

4. TITLE AND SUBTITLE
Radiologist Evaluation of DEI Breast Specimen Imaging

5. FUNDING NUMBERS
DAMD17-99-1-9330

6. AUTHOR(S)
Etta Pisano, M.D.

7. PERFORMING ORGANIZATION NAME(S) AND ADDRESS(ES)
University of North Carolina
Chapel Hill, North Carolina 27599-7510

E-MAIL:
etpisano@med.unc.edu

8. PERFORMING ORGANIZATION REPORT NUMBER

9. SPONSORING / MONITORING AGENCY NAME(S) AND ADDRESS(ES)
U.S. Army Medical Research and Materiel Command
Fort Detrick, Maryland 21702-5012

10. SPONSORING / MONITORING AGENCY REPORT NUMBER

11. SUPPLEMENTARY NOTES

12a. DISTRIBUTION / AVAILABILITY STATEMENT
Approved for public release; distribution unlimited

12b. DISTRIBUTION CODE

13. ABSTRACT ***(Maximum 200 Words)***

The specific aims of this proposal are to determine the acquisition parameter values for obtaining the best DEI images for breast imaging. There are numerous parameter values for collection of DEI images and design specifications of a compact source for breast imaging depend upon what these values are. During the first year of this grant, we have acquired images of three tissue specimens at all the above parameter values except at Si(5,5,5). We have pathology assessments of the tissue samples and have identified 10 regions of interest for the readers to evaluate. We have the image processing algorithms ready for use including PLAHE, a new version of CLAHE (contrast limited adaptive histogram equalization). We have downloaded all the synchrotron images to our lab at UNC and have finished reformating them for display on our systems. An observer study is proposed and will begin within the next three months which will allow expert radiologists to score DEI images obtained with different acquisition parameter values. From this study, we can determine the optimal design specifications for a clinically useful breast imaging system.

14. SUBJECT TERMS	15. NUMBER OF PAGES
Breast Cancer	13
	16. PRICE CODE

17. SECURITY CLASSIFICATION OF REPORT	18. SECURITY CLASSIFICATION OF THIS PAGE	19. SECURITY CLASSIFICATION OF ABSTRACT	20. LIMITATION OF ABSTRACT
Unclassified	Unclassified	Unclassified	Unlimited

FOREWORD

Opinions, interpretations, conclusions and recommendations are those of the author and are not necessarily endorsed by the U.S. Army.

___ Where copyrighted material is quoted, permission has been obtained to use such material.

___ Where material from documents designated for limited distribution is quoted, permission has been obtained to use the material.

___ Citations of commercial organizations and trade names in this report do not constitute an official Department of Army endorsement or approval of the products or services of these organizations.

N/A In conducting research using animals, the investigator(s) adhered to the "Guide for the Care and Use of Laboratory Animals," prepared by the Committee on Care and use of Laboratory Animals of the Institute of Laboratory Resources, national Research Council (NIH Publication No. 86-23, Revised 1985).

X For the protection of human subjects, the investigator(s) adhered to policies of applicable Federal Law 45 CFR 46.

N/A In conducting research utilizing recombinant DNA technology, the investigator(s) adhered to current guidelines promulgated by the National Institutes of Health.

N/A In the conduct of research utilizing recombinant DNA, the investigator(s) adhered to the NIH Guidelines for Research Involving Recombinant DNA Molecules.

N/A In the conduct of research involving hazardous organisms, the investigator(s) adhered to the CDC-NIH Guide for Biosafety in Microbiological and Biomedical Laboratories.

Etta D. Orso 6/21/00

PI - Signature Date

Table of Contents

Cover..... 1

SF 298..... 2

Foreword..... 3

Table of Contents..... 4

Introduction..... 5

Body..... 5

Key Research Accomplishments..... 6

Reportable Outcomes..... 6

Conclusions..... 6

References..... 6

Appendices..... 6

5. Introduction

The purpose of this study is to determine which physical operating characteristics for obtaining DEI images provide the optimum image for breast cancer imaging. This determination will be based on expert observer studies. The results will then be used as the design specifications for a compact source. The specific aims of this proposal are to determine the physical characteristics of the acquisition of DEI images for breast imaging. There are numerous parameter values for collection of DEI images and design specifications of a compact source for breast imaging depend upon what these values are. An observer study is proposed which will allow expert radiologists to score DEI images obtained with different acquisition parameter values. From this study, we can determine the optimal design specifications for a clinically useful breast imaging system.

6. Body

There are many different acquisition parameters that can effect the data that are used to form the DEI image. We propose the following parameters to be evaluated:

1. Two crystal types: Bragg – reflection from the "analyzer" crystal
   Laue – transmission through the "analyzer" crystal
2. Three reflection types to establish optimal refraction and scatter rejection contrast.
   Si(1,1,1), Si(3,3,3), Si(5,5,5) See definitions Appendium A.
3. Three imaging energies: 18, 25, and 30 keV.
4. Five locations on the rocking curve (±1 Darwin width, ±½ Darwin width, and at the analyzer peak) plus a radiograph (image without analyzer).
5. Two image processing methods. PLAHE and MIW.

During the first year of this grant, we have acquired images of three tissue specimens at all the above parameter values except at Si(5,5,5). This configuration can not be accomplished with the present equipment available to us. We will continue to address this issue, but the decision was made to progress with the reader study with the data we have acquired.

We have pathology assessments of the tissue samples and have identified 10 regions of interest for the readers to evaluate. We have the image processing algorithms ready for use including PLAHE, a new version of CLAHE (contrast limited adaptive histogram equalization).

We have downloaded all the synchrotron images to our lab at UNC and have finished reformating them for display on our systems.

We are presently working out the details of the reader study, how many readers, what display scheme to use, etc. We expect to begin the reader study sometime this summer.

7. Key research accomplishments

- Acquired images with synchrotron at all parameter values for three breast tissue specimens.
- Completed pathology for all specimens.
- Reformated images for display at UNC.
- Two image processing algorithms completed and ready to apply.

8. Reportable Outcomes.

None at this point in time.

9. Conclusions

The purpose of this study is to determine what acquisition parameter values produce the best DEI images. At the end of the first year we have acquired images for all the parameter values proposed except for the Si(555) crystal configuration. We have modified our goals to not include this configuration at this time, due to technical difficulties that would keep us from proceeding in a timely manner.

We have added a set of acquisition images that will determine the necessity of breast compression, or at what level of compression is needed. Both image sets are presently being assembled for the reader study.

The results of the reader study should determine which parameter values should be used to acquire the image and what level of compression is needed, if any.

10. References

None.

11. Appendices

Pisano ET, Johnston RE, Chapman D, Geradts J, Iacocca MV, Washburn DB, Sayers DE, Zhong Z, Kiss, MZ, Thomlinson WC. Radiology 2000; 214: 895-901

Human Breast Cancer Specimens: Diffraction-enhanced Imaging with Histologic Correlation—Improved Conspicuity of Lesion Detail Compared with Digital Radiography[1]

Etta D. Pisano, MD
R. Eugene Johnston, PhD
Dean Chapman, PhD
Joseph Geradts, MD
Mary V. Iacocca, MD
Chad A. Livasy, MD
David B. Washburn, PhD
Dale E. Sayers, PhD
Zhong Zhong, PhD
Miklos Z. Kiss, MS
William C. Thomlinson, PhD

Index terms:
Breast radiography, technology, 00.119
Synchrotron

Radiology 2000; 214:895–901

[1] From the Departments of Radiology (E.D.P., R.E.J., D.B.W.) and Pathology (M.V.I., C.A.L.) and the UNC-Lineberger Comprehensive Cancer Center (E.D.P.), University of North Carolina School of Medicine, Manning Dr, Chapel Hill, NC 27599-7510; the Department of Physics and Center for Synchrotron Radiation Research and Instrumentation, Illinois Institute of Technology, Chicago (D.C.); the Nuffield Department of Pathology and Bacteriology, University of Oxford, United Kingdom (J.G.); the Department of Physics, North Carolina State University, Raleigh (D.E.S., M.Z.K.); the Brookhaven National Laboratory, Upton, NY (Z.Z.); and the European Synchrotron Radiation Facility, Grenoble, France (W.C.T.). Received February 1, 1999; revision requested March 31; final revision received June 25; accepted July 20. Supported in part by U.S. Army grant DAMD 17-96-1-6143, by the National Synchrotron Light Source at Brookhaven National Laboratory under U.S. Department of Energy contract DE-AC 02-76CH00016, and by the State of Illinois Higher Education Cooperative Agreement. **Address reprint requests to** E.D.P. (e-mail: *etpisano@med.unc.edu*).

Author contributions:
Guarantors of integrity of entire study, E.D.P., R.E.J.; study concepts, E.D.P., R.E.J., D.C., D.B.W., D.E.S., W.C.T.; study design, E.D.P., R.E.J., D.C.; definition of intellectual content, E.D.P., R.E.J., D.C.; literature research, E.D.P., R.E.J., D.C.; experimental studies, E.D.P., R.E.J., D.C., J.G., C.A.L., D.B.W., D.E.S., Z.Z., M.Z.K., W.C.T.; data acquisition, R.E.J., D.C., D.B.W., D.E.S., Z.Z., M.Z.K., W.C.T.; data analysis, E.D.P., R.E.J., J.G., M.V.I., C.A.L.; manuscript preparation, E.D.P., R.E.J., D.C., C.A.L., M.V.I., J.G., Z.Z.; manuscript editing and review, all authors.

Seven breast cancer specimens were examined with diffraction-enhanced imaging at 18 keV with a silicon crystal with use of the silicon 333 reflection in Bragg mode. Images were compared with digital radiographs of the specimen, and regions of increased detail were identified. Six of the seven cases (86%) showed enhanced visibility of surface spiculation that correlated with histopathologic information, including extension of tumor into surrounding tissue.

Mammographic technology has improved dramatically in the past 2 decades. Improvements include the development of dedicated mammographic equipment with appropriate x-ray beam quality, adequate breast compression, and automatic exposure control (1). Digital mammography is the most recent development and is now being introduced into the clinic, with the promise of improved early detection of breast cancer (2). All currently existing systems depend on the depiction of x-ray absorption to define the differences between normal and abnormal tissues. A radiographic imaging method, diffraction-enhanced imaging partly depends on the refractive properties of an object in the creation of a scatter-free image (3). Use of this method, which improves the x-ray beam properties for enhanced contrast and currently available digital mammographic detectors, could increase early detection of occult disease. See the Appendix for a complete description of the principles of diffraction-enhanced imaging.

Other researchers have applied diffractive optics to imaging problems (4–7) and have observed refraction effects. There is also interest in phase-contrast imaging that makes use of the high transverse coherence of third-generation synchrotron sources. However, these types of measurements are limited to use with materially thin objects or high x-ray imaging energies to obtain phase-contrast images of the object (8,9). The diffraction-enhanced imaging technique is successful with samples of the same thickness as the human breast and, after further development, should be possible without the use of a synchrotron.

For this project, the mammographic technique under development makes use of the high intensity and collimation of synchrotron radiation to create a monoenergetic line scanning system with very little scatter (10). Synchrotron radiation is the electromagnetic radiation emitted as charged particles (electrons or positrons) change direction while passing through electromagnets. The magnets restrain the particles to a circular orbit in large accelerators called "synchrotrons," although most of the modern machines are really storage rings in which the electric currents persist for many hours at constant energy. The particles are highly relativistic, traveling at or near the speed of light, so that the radiation produced has several unique properties. The inten-

sity of the radiation is five to six orders of magnitude higher than that of a laboratory source. The energy spectrum is smooth and continuous from the infrared to the hard x-ray range. The radiation is inherently collimated in the plane of the orbit. The radiation is emitted from the machine through metal windows and delivered to experimental stations through long vacuum vessels. These tubes are called beam lines. The unique radiation properties, when coupled with modern perfect crystal x-ray optics, are used to define very high intensity beams that are highly monochromatic at any selected energy and are highly collimated for medical and other applications.

In addition, an analyzer crystal was used in this study as a scatter rejection optic.

Herein, we describe our first results with imaging of human breast cancer specimens. We have previously reported our results with phantoms (10).

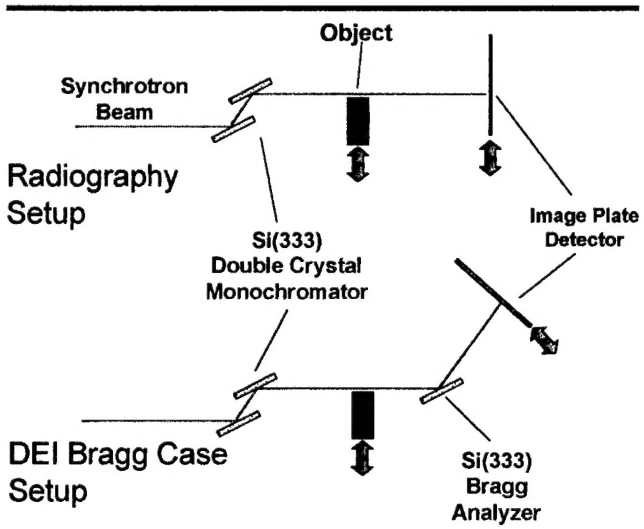

Figure 1. Schematic of experimental setup. At the top, synchrotron setup used to obtain radiographs of the object, in this case, breast specimens, is shown. At the bottom, addition of the analyzer crystal (Bragg or reflection geometry) used to implement the diffraction-enhanced imaging (*DEI*) system is shown.

Materials and Methods

The experimental setup used to apply this technique is shown in Figure 1, which shows both the synchrotron radiographic system and the addition of the analyzer crystal to the diffraction-enhanced imaging system. The white synchrotron beam is made nearly monochromatic by using a silicon double-crystal monochromator. For the measurements in this study, the beam energy was either 18 or 30 keV. Experiments were performed at two facilities: the National Synchrotron Light Source (Brookhaven National Laboratory, Upton, NY) with use of the X27C Research and Development Group beam line, and the Advanced Photon Source (Argonne National Laboratory, Argonne, Ill) with use of the 1-BM, or bending magnet, beam line of the Synchrotron Radiation Instrumentation Collaborative Access Team. This study was formally granted an exemption from review by the institutional review board at the participating institutions.

The imaging beam was approximately 80 mm wide and 1 mm high at the location of the object. An ionization chamber was used to measure the radiation exposure at the surface of the object. Images with and those without the analyzer crystal were obtained at exposure levels comparable to those used in conventional mammographic x-ray systems. The breast specimen to be imaged was mounted on a scanning stage driven with a stepping motor. The x-ray beam transmitted through the object could be either imaged directly, as in standard radiography, or after diffraction in the vertical plane by means of the silicon crystal analyzer. Radiation exposure to the image plate was controlled by adjusting the scanning speed and absorbers in the incident beam to maintain an exposure of about 1.3 C/kg (5 mR) to the plate. Typical scanning times for these experiments were on the order of 4–200 seconds. These limits were dictated by our scanning motors and the mechanical system.

The detector was a photostimulable phosphor image plate typically used for radiologic examinations (models HR5 [high spatial resolution] and ST5 [standard spatial resolution]; Fuji Medical Systems USA, Stamford, Conn). The image recorded on the plate was digitized, stored, and displayed with a reader and workstation (model AC3; Fuji Medical Systems) or with a reader system (model BAS2000; Fuji Medical Systems). The image plates were read with a 2,560 × 2,048 matrix, which resulted in an image with 100 μm per pixel (0.1 × 0.1 mm).

The diffraction angle of the analyzer crystal could be finely tuned by using a stepper-motor driven translation stage to push on a long bar attached to an axle to which the crystal was attached (tangent arm). The spatial resolution limit of the tangent arm was 0.1 μradian, which was sufficient for placing the Bragg analyzer crystal at a selected position on its rocking curve.

For each sample, a "normal" radiograph with the monochromatic beam could be obtained by moving the image plate to a location just downstream of the object on the sample scanning stage and imaging the combined object and image plate through the fan beam. Diffraction-enhanced images were then acquired with the analyzer crystal tuned to various positions on the rocking curve by translating the sample and the image plate in opposite directions at the same speed through the fan beam. The change in scanning direction arises from the beam inversion from the analyzer crystal. At a scanning speed of about 10 mm/sec, the surface dose on the sample was a few milligray at 18 keV and 10ths of a milligray at 30 keV. Rocking curves through a specific location within the specimen were obtained by fixing the specimen in the fan beam and performing a series of exposures by incrementally changing the position of the analyzer crystal and the vertical position of the image plate.

Seven formalin-fixed human breast cancer specimens were imaged, three infiltrative lobular and four infiltrating ductal carcinomas. These specimens were approximately 1 cm thick. Each biologic sample was sealed in a plastic bag and compressed between two Lucite plates so that the absorbing thickness was approximately 40 mm. Images were obtained at 18 keV by using the reflection of silicon 333 crystals as monochromator and analyzer. The crystals were in symmetric Bragg mode, meaning that the beam made the same angle with the crystal surface. For each sample, five images were obtained at

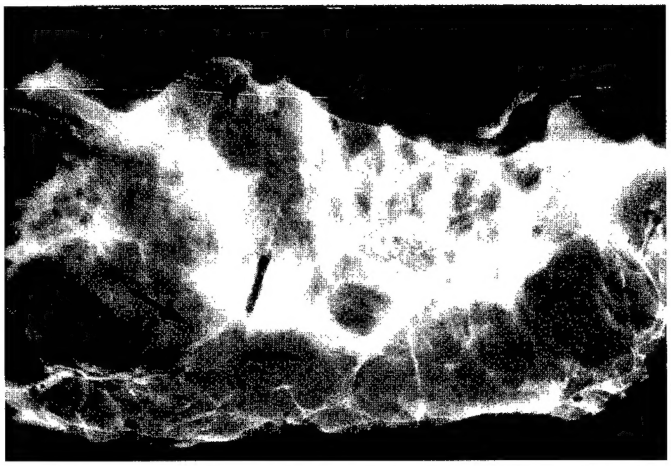

a.

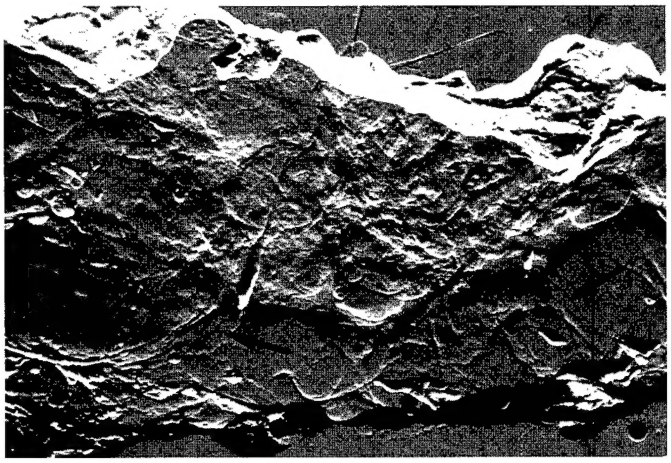

b.

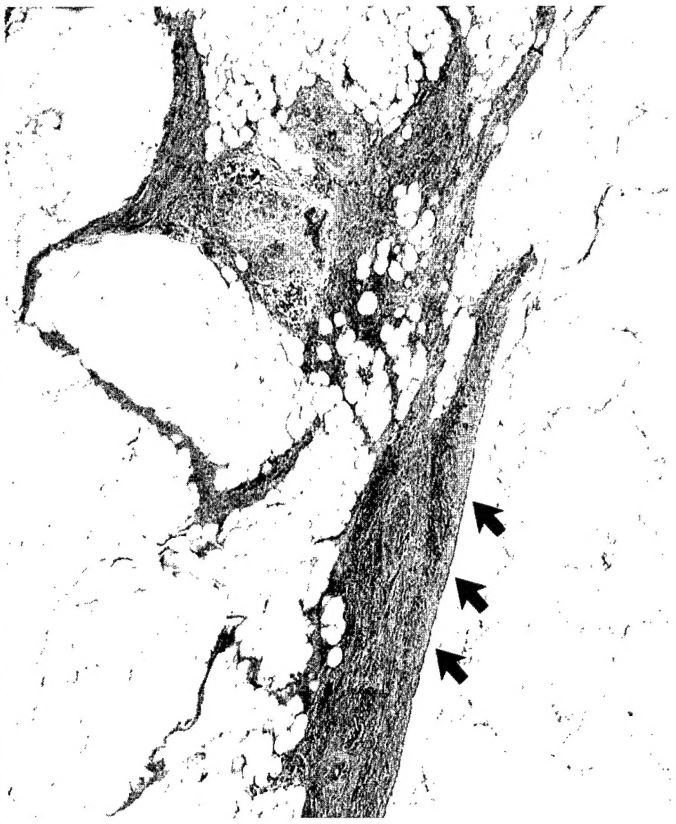

c.

Figure 2. Specimen with invasive lobular carcinoma, which typically grows in single files of cells. **(a)** Digital radiograph of the specimen. Note the vague linear densities along the inferior margin of the lesion, some of which are marked with arrows. A scratch artifact lies across the top portion of the image. **(b)** Diffraction-enhanced image of the same specimen. Note the increased prominence and number of lines that extend from the inferior border of the lesion at the arrows. **(c)** Photomicrograph of the spiculations identified between the two arrows on the left in **b** shows a band of fibrous tissue with invasive lobular carcinoma (arrows). The other spiculations identified by the single arrow on the right in **b** proved to be both infiltrating lobular carcinoma and fibrous bands. (Hematoxylin-eosin stain; original magnification, ×10.)

angular positions of 0 (peak position), $\pm W/2$, and $\pm W$ on the rocking curve, where W is the full-width at half maximum point on the rocking curve.

Images of the same specimens were also obtained with use of a digital mammographic unit (SenoScan; Fischer Medical Imaging, Boulder, Colo).

Diffraction-enhanced and digital images of the specimens were subsequently evaluated by one experienced breast imager (E.D.P.). She identified regions of interest within the diffraction-enhanced images that showed apparently increased lesion information, for example, areas of increased surface spiculation. This was done by comparing the digital radiograph and the diffraction-enhanced image side by side and circling areas on the latter. No regions of interest were identified on the standard digital radiographs.

Histologic whole-mount slides of the specimens were made. With the assistance of the radiologist and direct comparison of the whole-mount slides to the diffraction-enhanced images of the specimen, an experienced breast pathologist (J.G.) evaluated the regions of interest in the specimens to determine whether the information apparent on the diffraction-enhanced images correlated with real histopathologic structures.

Results

Visualization of lesion spiculation and architectural distortion of the breast cancer specimens improved on diffraction-enhanced images in six of seven cases (86%) on the basis of the 10 regions of interest identified by the participating radiologist. These regions of interest were areas that showed increased spiculation or architectural distortion on the diffraction-enhanced image compared with on the standard digital radiograph of the specimen. For these 10 areas, histopathologic review revealed the spiculations to be infiltrating ductal carcinoma (two regions in one specimen), infiltrating lobular carcinoma (two regions, each in a different specimen), ductal carcinoma in situ with surrounding fibrosis (one region), fibrosis alone (three regions in one specimen), fibrocystic change (one region), and biopsy site changes (one region). In every case of enhanced spiculation visualization, there was a histopathologic correlate that could explain the imaging finding.

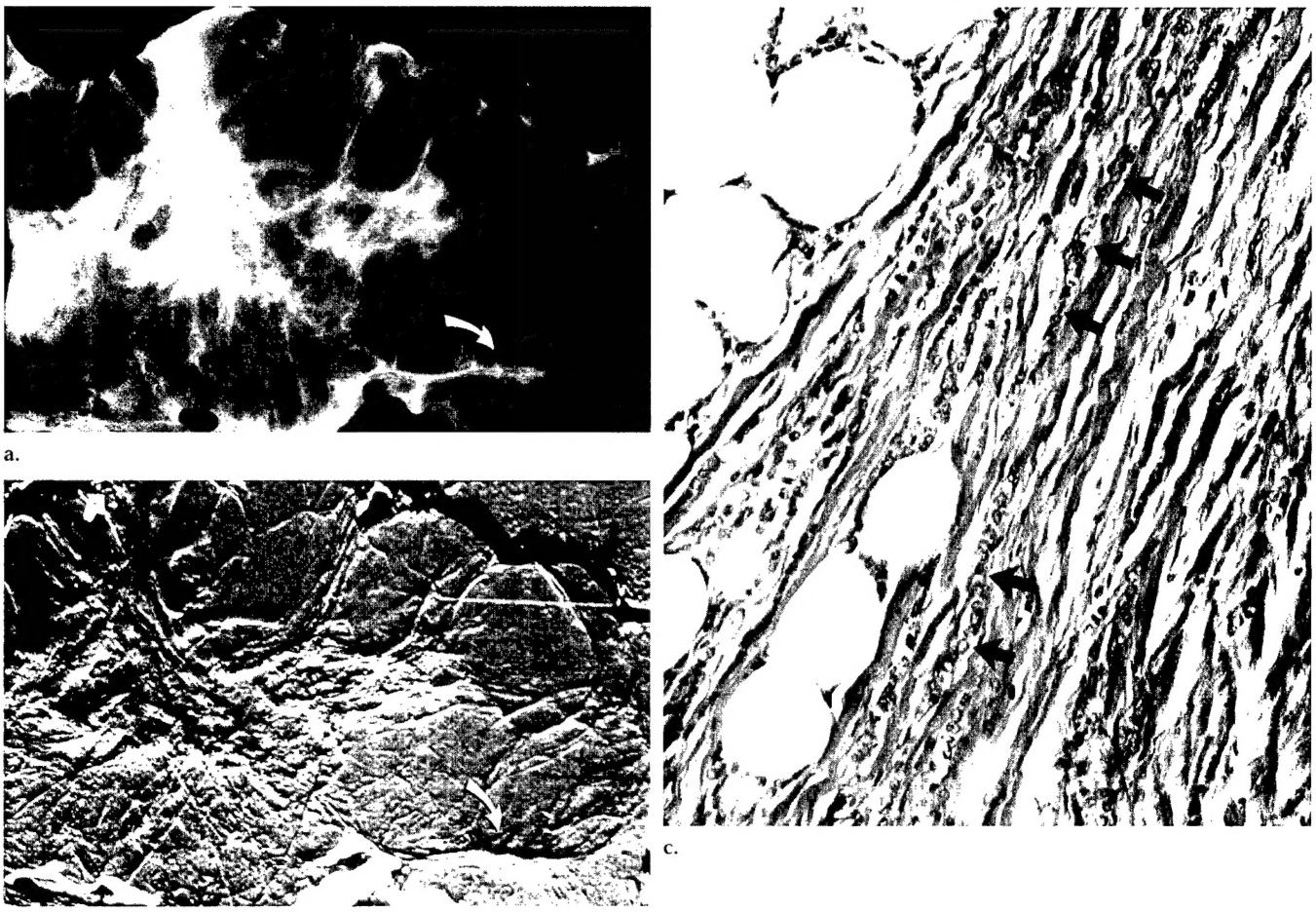

Figure 3. (a) Digital radiograph of the specimen shows invasive lobular carcinoma that extends to the edge. As marked with an arrow, there is a suggestion of an additional focus of tumor with some evidence of spiculations that extend from its surface at the edge of the specimen. (b) Diffraction-enhanced image shows improved visibility of these fine lines (arrow). This was identified as a region of interest for this study. (c) Photomicrograph reveals invasive lobular carcinoma (arrows) within fibrous bands, which correspond to the visualized spiculations. (Hematoxylin-eosin stain; original magnification, ×100.)

The figures show the improved depiction of spiculations corresponding with tumor extension (Figs 2–4) and with fibrosis (Fig 5).

Discussion

This technique was developed with use of a synchrotron x-ray source. The high intensity, collimation, and tunability available with use of synchrotron sources make them ideal environments in which imaging technologies, such as diffraction-enhanced imaging, can be developed. An obvious drawback is the translation of this technology to more conventional x-ray sources in a laboratory or clinical environment. The diffraction-enhanced imaging technique delivers x-ray exposures to tissue and phantoms that is similar to that delivered by conventional x-ray mammographic units. The difficulty arises in generating the highly collimated, monoenergetic imaging beam. The monochromating crystal and analyzer crystal must use the same Bragg reflection to achieve the high degree of collimation necessary to observe the refraction and scatter rejection presented earlier. Perfect single-crystal silicon monochromators and analyzers are used to achieve the diffraction-enhanced imaging effect. Such systems are used routinely with conventional x-ray sources, but for diffraction-enhanced imaging to be applied to mammography, the source intensity and properties must be such that exposures are obtained in a few seconds to avoid image blurring due to patient motion.

Estimates of the flux from conventional x-ray sources have yielded scanning time estimates of approximately 1,000–10,000 seconds. Clearly, such long scanning times to deliver a diffraction-enhanced image set would be unacceptable. These times are based on commercially available x-ray sources and indicate that the application of diffraction-enhanced imaging with conventional sources will be challenging. However, there are reasons to believe that this will be possible.

First, conventional x-ray imaging makes use of an x-ray beam that arises directly from the target of the x-ray tube. The spectrum may be filtered. In the implementation of diffraction-enhanced imaging, a monochromator must be used to collimate the imaging beam. This monochromating element allows the operational parameters of the tube to be optimized for the creation of the flux at the desired imaging energy. This eliminates concern for other parts of the spectrum that would normally deliver unnecessary dose, for example, the creation of bremsstrahlung radiation. Use of high accelerating voltages becomes attractive since the flux con-

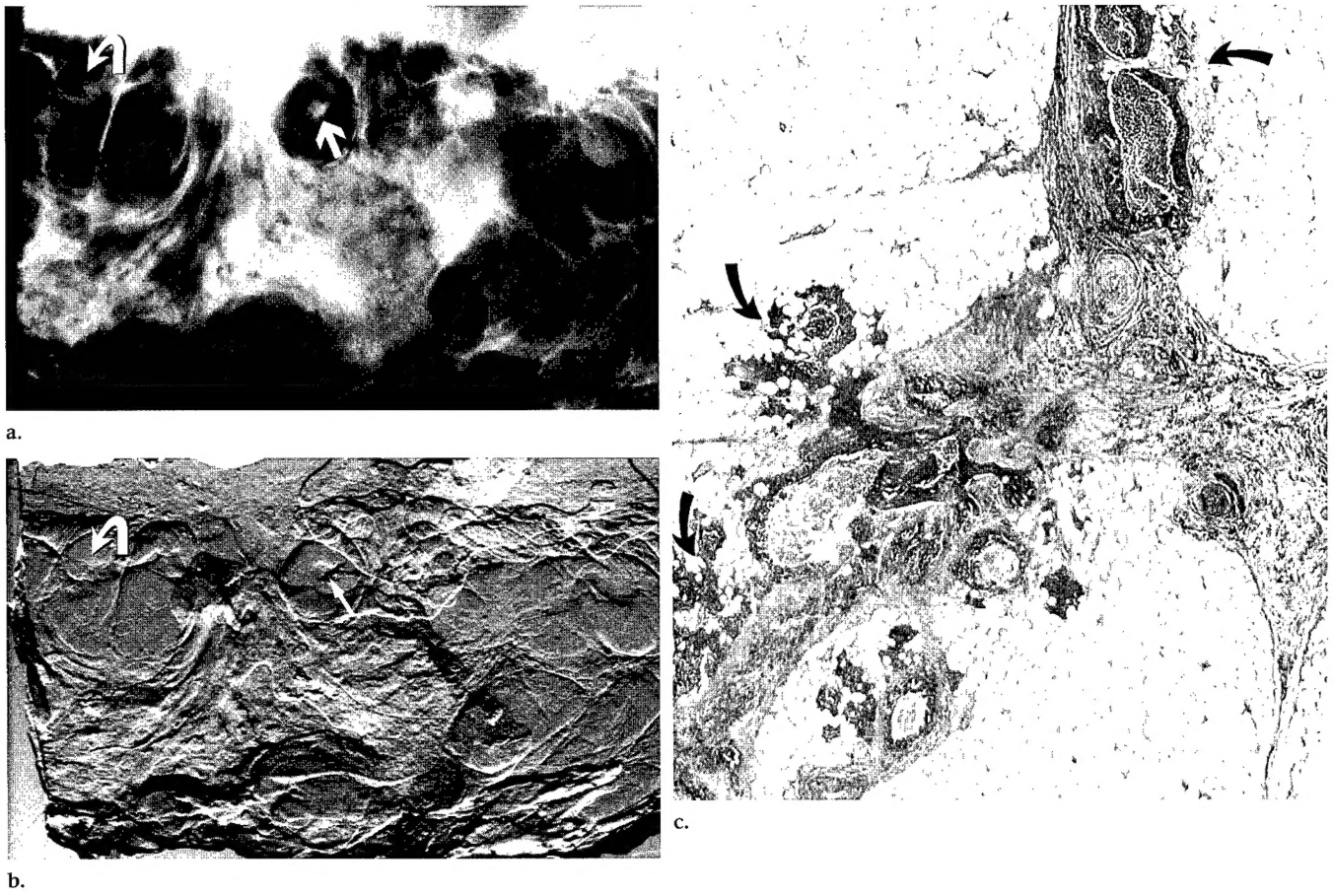

Figure 4. **(a)** Digital radiograph of the specimen for an infiltrating ductal carcinoma that extends to the skin. The curved arrow in **a** indicates an area identified as a region of interest for this study that appears as a possible mass or satellite lesion. The straight arrow indicates a small mass. **(b)** Diffraction-enhanced image of the specimen with the area corresponding to the marked area in **a** indicated with a curved arrow. This reveals subtle spiculations along the superior aspect of a definite mass. In addition, at the mass marked with a straight arrow, there are more obvious spiculations than are seen in **a**. These proved to be a focus of infiltrating ductal carcinoma. **(c)** Photomicrograph reveals tongues of infiltrating ductal carcinoma (arrows) that correspond to the subtle spiculations visible at the tip of the curved arrow in **b**. (Hematoxylin-eosin stain; original magnification, ×5.)

tained in the emission from the source is enhanced at higher accelerating voltages.

Second, the prospect of obtaining diagnostic information from the diffraction image leads to higher optimal imaging energies. Since the tissue absorption is reduced at higher energy, the transmission and thus flux requirements are reduced. However, two competing effects limit the imaging energy. First, the refraction sensitivity is reduced; second, the flux diffracted by the monochromator is reduced. Estimates and measurements indicate that the optimal imaging energy is in the range of 30 keV. An additional benefit of this energy is reduced dose delivery (15 times less than that at 18 keV) and possible reduction in breast compression.

Finally, the advent of digital detectors for mammography may allow more efficient use of exposure. A contributing element may also be the lack of scatter in the acquired image, which may allow a reduction in exposure in the acquisition of useful diagnostic information. Perhaps this method, paired with more efficient detectors, will allow use of higher energy beams and lower patient dose.

The combination of these four factors may allow construction of a nonsynchrotron, conventional source. However, determination of the optimal parameters for a conventional system will take time. The synchrotron, with its wide flexibility in the trial and modeling of source parameters, will play a major role in this endeavor.

These results suggest that there is potential for improved visualization of breast cancer detail with use of the diffraction component of the x-ray beam. This improved detail was achieved without optimization of this technique for breast imaging. To obtain the maximum amount of information on diffraction-enhanced images for breast cancer detection and characterization, careful evaluation of image detail with histologic correlation by experts should be carried out. In this manner, the optimal crystal type, reflection type, imaging energy, and rocking curve location can be determined so that the specifications for a clinically useful (office-based) system can be developed.

Given the increased visibility of lesion features with diffraction-enhanced imaging in all three cases of infiltrating lobular carcinoma that we evaluated, we believe this method might improve detectability of this frequently occult lesion. Infiltrating lobular carcinoma is the second most common type of invasive breast cancer, occurring in approximately 15% of women with infiltrative tumors. In fact, lobular tumors are bilateral in 10% of cases. Frequently, the extent of this type of tumor is underestimated with traditional imaging methods. Perhaps diffrac-

tion-enhanced imaging can improve the detection of this lesion by increasing the visibility of subtle spiculations and architectural distortions.

This study is limited in that we have yet to evaluate any specimens that predominantly contain clustered calcifications. We are currently imaging breast samples that contain this type of mammographic lesion. In addition, this study is essentially qualitative, and no images of normal control tissue or benign lesions were evaluated. A clinically realistic analysis of the potential benefits of this technique will require the imaging of a wider set of sample types and ultimately of patients.

In summary, we believe that these preliminary results suggest promise for diffraction-enhanced imaging as applied to breast cancer detection and diagnosis. Further studies are needed to determine the optimal diffraction-enhanced imaging parameters for these clinical tasks.

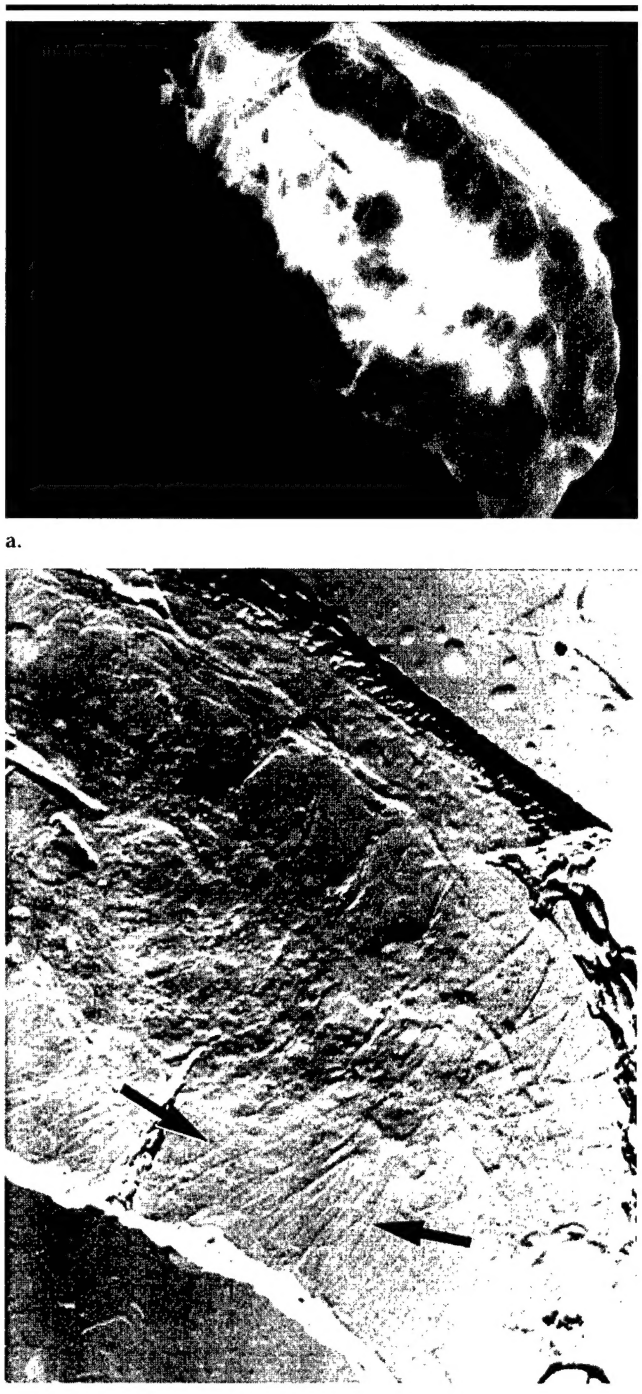

Figure 5. (**a**) Digital radiograph of a specimen of infiltrating ductal cancer. (**b**) Diffraction-enhanced image shows fine spiculations on the surface of the lesion, between the two arrows, that are not seen in **a**. This area was identified as a region of interest for this study. At pathologic examination, the area represented only fibrous tissue bands, a desmoplastic reaction to the presence of tumor. This pathologic feature is a frequent cause of spiculations and architectural distortion on mammograms.

Appendix

Principles of Diffraction-enhanced Imaging

In conventional radiography, an area beam is used that, after traversing and interacting with the subject, is intercepted and recorded by an area detector. The interaction of x rays with the subject is complex, involving absorption, refraction (4–7), and scattering. The scattering may include small-angle scattering (11) (scattering angles less than milliradians) that carries information about the subject's structure on the length scale as large as micrometers. This information is lost in normal radiography because of its small-angle nature. The refraction of x rays inside the object is also not detectable at conventional radiography owing to its small-angle nature (on the order of microradians).

X-ray diffraction from perfect crystals, with narrow reflection angular width (on the order of a few microradians) and peak reflectivity of close to unity, provides the tools necessary to prepare and analyze x-ray beams that traverse an object on the microradian scale (12). Such crystals, typically silicon, are routinely used in the semiconductor industry to make integrated circuits and electronic devices. The purity and perfection of these crystals have allowed many advances in x-ray diffraction techniques, in particular at x-ray synchrotron sources.

The condition for x-ray diffraction from a crystal is met only when the incident beam makes the correct angle to the atomic lattice planes in the crystal for a given x-ray energy or wavelength. When this condition is met, the beam diffracts from the planes over a narrow range of incident angles, so-called Bragg diffraction. As the crystal is rotated about an axis parallel to the lattice planes and perpendicular to the incident beam direc-

tion, an intensity variation is observed. This is referred to as the "rocking curve." The shape of this curve is roughly triangular, with the peak reflectivity approaching nearly 100%.

In diffraction-enhanced imaging, an imaging beam is prepared by means of diffraction of the polychromatic beam from the synchrotron to create a nearly monoenergetic imaging beam. This beam is then passed through the object being imaged as in conventional radiography. However, a matching crystal is placed between the object and the detector. This crystal is set at or near the peak of Bragg diffraction and is called the analyzer crystal. A schematic representation of a synchrotron radiography and diffraction-enhanced imaging system is shown in Figure 1.

Since the condition for diffraction from this crystal limits the x rays that can be diffracted into the detector, it automatically provides a high degree of scatter rejection, which results in improved image contrast. The range of angles accepted by the analyzer crystal is a few microradians, which thus provides scatter rejection more completely than does the capabilities of conventional antiscatter techniques such as slit collimation and grids.

The rejected scatter falls into a category referred to as "small-angle scattering" (13), or scattering that arises from diffraction from very small, organized structures. This scattering intensity, which would normally appear on the image, is missing and appears as does absorption on the image. We call the improved image contrast obtained by means of scatter rejection of this sort "extinction contrast," which is drawn from a similar term used in optics and x-ray diffraction to describe intensity loss due to diffraction and scattering. Therefore in diffraction-enhanced imaging, the image that represents the absorption of the object by x rays is referred to as the "apparent absorption image," since it has contrast derived from both absorption and scatter rejection, or extinction.

The shape of the rocking curve of the analyzer crystal introduces a sensitivity to refraction that occurs within the object when the analyzer crystal is detuned from the peak position. Density, thickness, or material variations in an object will refract the x rays as they cross through the material. These small angular variations are generally in a range smaller than a microradian. The steep sides of the reflectivity curve convert these subtle angle variations into intensity variations, which thus makes refraction effects visible on an image. In this study, we found that by acquiring an image pair with the analyzer crystal set to diffract on each side of the rocking curve, we can separate refraction effects from combined absorption and extinction effects (3,14).

Thus, the diffraction-enhanced imaging technique introduces two sources of image contrast to radiography: refraction and extinction (3). Each of these image contrast sources may be further developed to apply to medical and biologic imaging.

Glossary of Terms

Analyzer crystal.—A crystal that is placed in the x-ray beam that emerges from the target material and is used to reflect the x-ray beam at the Bragg angle onto the detector.

Bragg angle.—The angle θ at which an electromagnetic beam is incident to and reflected from a crystal plane. The relationship between the wavelength, λ, the distance between the crystal planes, d, and the angle of reflection, θ, is given with the Bragg equation: $\lambda = 2d \sin \theta$.

Diffraction.—A change in direction of an x ray when it is incident on a substance that has a periodic structure at the molecular level.

Extinction.—A term used in x-ray optics to describe the loss of intensity from an x-ray beam owing to the scattering of photons out of the beam at very small angles, primarily because of diffraction effects.

Reflection.—The changing of direction of an electromagnetic beam when it is incident on the surface of a plane. The reflection angle is equal but opposite in direction to the incident angle.

Refraction.—A change in direction of the electromagnetic beam when it passes obliquely across a boundary between two materials in which the velocity of propagation is different. This can also occur in a single medium owing to variations in its physical properties.

Rocking curve.—The intensity of the x-ray beam that is reflected from the analyzer crystal as the analyzer angle θ is varied above and below the Bragg angle that corresponds to the incident beam. The intensity of the reflected beam varies correspondingly from zero to a maximum (at the Bragg angle) and to zero again.

Synchrotron radiation.—Electromagnetic radiation emitted as the path of a charged particle (an electron or positron) is bent as it passes through a magnetic field.

Acknowledgments: The authors acknowledge the contributions of Anna Cleveland of the University of North Carolina at Chapel Hill, Nicholas F. Gmur, MS, of the Brookhaven National Laboratory, Fischer Medical Imaging (Boulder, Colo), Fuji Medical Systems USA (Stamford, Conn), and Eastman Kodak (Rochester, NY).

References

1. Haus AG. Technologic improvements in screen-film mammography. Radiology 1990; 174:628–637.
2. Shtern F. Digital mammography and related technologies: a perspective from the National Cancer Institute. Radiology 1992; 183:629–630.
3. Chapman D, Thomlinson W, Johnston RE, et al. Diffraction enhanced x-ray imaging. Phys Med Biol 1997; 42:2015–2025.
4. Ingal VN, Beliaevsky EA. X-ray plane-wave topography observation of phase contrast from a non-crystalline object. J Phys 1995; 28:2314–2317.
5. Somenkov VA, Tkalich AK, Shil'shtein SS. Refraction contrast in x-ray introscopy. Sov Phys Tech Phys 1991; 36:1309–1311.
6. Podurets KM, Somenkov VA, Shil'shtein SS. Refraction-contrast radiography. Sov Phys Tech Phys 1989; 34:654–657.
7. Gureyev TE, Wilkins SW. Regimes of x-ray phase-contrast imaging with perfect crystals. Il Nuovo Cimento 1997; 19:545–552.
8. Davis TJ, Gureyev TE, Gao D, Stevenson AW, Wilkins SW. X-ray image contrast from a simple phase object. Phys Rev Lett 1995; 74:3173–3175.
9. Davis TJ, Gao D, Gureyev TE, Stevenson AW, Wilkins SW. Phase-contrast of weakly absorbing materials using hard x-rays. Nature 1995; 373:595–598.
10. Johnston RE, Washburn D, Pisano E, et al. Mammographic phantom studies with synchrotron radiation. Radiology 1996; 200:659–663.
11. Bushuev VA, Ingal VN, Belyaevskaya EA. Dynamical theory of images generated by noncrystalline objects for the method of phase-dispersive introscopy. Crystallography Reports 1966; 41:766–774.
12. Zachariasen WH. X-ray interference in real crystals. In: Theory of x-ray diffraction in crystals. New York, NY: Wiley, 1945; chap 4.
13. Guinier A, Fournet G, Walker CB, Yudowitch KL. Small-angle scattering of x-rays. New York, NY: Wiley, 1955.
14. Chapman D, Thomlinson W, Arfelli F, et al. Mammography imaging studies using a Laue analyzer crystal. Rev Sci Instrum [serial on CD-ROM]. 1996; 67:3360–3365.